Laser-induced decomposition of HNS at 263nm

YI SUN*, YEWEI XU
Engineering Research Center of Biomass Materials, Ministry of Education, School of Materials and Chemistry, Southwest University of Science and Technology, Mianyang, Sichuan, China

The laser-induced decomposition of solid HNS (2,2',4,4',6,6'-hexanitrostillbene) at 263 nm, induced by an 8-picosecond (ps) laser, has been studied by UV-Vis spectra, X-ray photoelectron spectroscopy (XPS) and mass spectra. The new peak at 310nm in UV-Vis spectra and the new peaks of N 1s XPS spectra at ~401 eV and O 1s XPS spectra at about ~528 eV suggest that a nitro-nitrite isomerization reaction with subsequent release of NO occurs in the decomposition process. Moreover, the appearance of 224m/z in mass spectra verifies that the fragmentation of trans-C=C bond takes place in the decomposition. The temperature risen within the irradiated sample volume has been calculated by integrating the heat conduction equation and the results show that there is a very low temperature rise of less than 40 K under our experimental conditions, which has been illustrated that the photochemical effect is the dominant reaction in the decomposition. The results will allow for better improvement of the stock reliability performance and detonation reaction process of HNS.

(Received December 2, 2021; accepted August 10, 2022)

Keywords: Laser-induce decomposition, HNS, Nitro-nitrite isomerization, The fragmentation of trans-C=C bond

1. Introduction

HNS (2,2',4,4',6,6'-hexanitrostillbene, see Fig. 1) is a typical heat-resistant and insensitive explosive with attractive characteristics of excellent thermal stability, impact, and shock insensitivity along with good performance. Laser initiation of high energetic explosive is a complex process, and the detonation mechanism that takes place during decomposition is not easily identified in chemical physics. The way of energy transferring from the laser beam to the localized bonds is yet not well understood. Exactly to say which bonds absorb the energy and results in molecules decomposition is also of great interests [1].

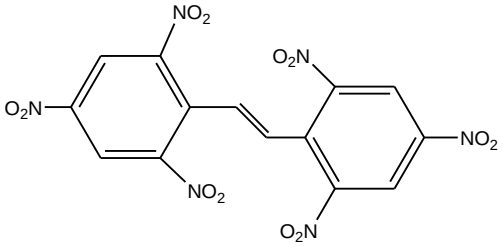

Fig. 1. The molecular structure of HNS

Up to now, the laser-induced decomposition of many energetic materials have been studied, including DMNA (dimethylnitramine) [2-4], TATB (1,3,5-triamino-2,4,6-trinitrobenzene) [5-9], HMX (1,3,5,7-tetranitro- 1,3,5,7-tetrazacyclooctane), RDX (1,3,5-trinitro-1,3,5-triaza cyclohexane) [10-15], CL-20 (2,4,6,8,10,12-hexanitro-2,4,6,8,10,12-hexaazaisowurtzitane) [13,16,17] and so on [18,19,20,21]. However, contradictory still exists for their photo-dissociation mechanisms. Among different mechanisms, C-NO_2 broken, O atom elimination, H atom transfer, OH formation and nitro-nitrite isomerization reaction *et al* have been proposed as the primary process under admittedly different experimental conditions, such as different phases, different temperatures, and different photoexcitation wavelengths. In 2013, we have reported that photodecomposition mechanism of 2,2',4,4',6,6'-hexanitrostillbene is wavelength-dependent [22]. However, no other related information for HNS has been reported in detail.

To further identify the photodecomposition mechanism of solid HNS at laser irradiation, we investigated the UV-Vis spectra, X-ray photoelectron spectroscopy and mass spectra of HNS irradiated before and after 263 nm in the present experiment. Moreover, we have calculated the temperature risen for the irradiated sample volume under our laser fluence to identify whether the decomposition is induced by thermal effect or photo effect.

2. Experiment section

HNS powder (with a purity > 99.5%) synthesized at the Institute of Chemical Materials is ground to a uniform grain size of 20 μm. The experimental arrangement of the photodecomposition experiment of HNS is shown in Fig. 2. The decomposition was achieved by focusing 263nm laser beam emitting from a Nd:YLF laser normal to the surface of the sample at a repetition rate of 10 Hz. The pulse duration is 8 ps (FWHM) and the peak power density is maintained at 10^8 W/cm^2 with a beam diameter of 3.2 mm. In the experiment, HNS powder was sandwiched between two quartz plates. The irradiated sample is then characterized by UV-Vis spectra, X-ray photoelectron spectroscopy, FT-IR spectra and Mass spectra.

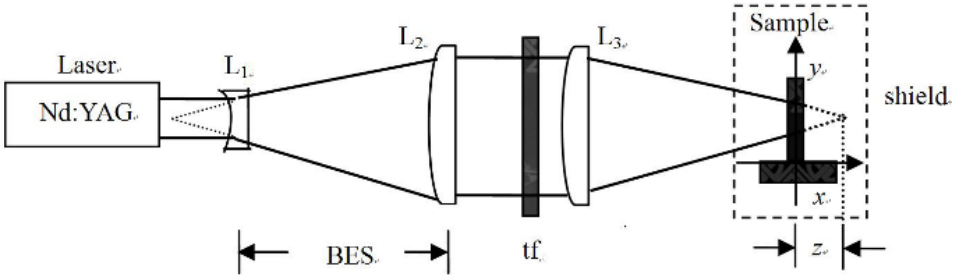

Fig. 2. Experimental arrangement of HNS photodecomposition. L_1, quartz plano-concave lens; L_2-L3, quartz plano-convex lenses; tf, neutral filters

3. Results

3.1. UV-Vis spectra

The UV-Vis spectra was carried out in acetonitrile and registered in VARIAN CARY 100 UV-Vis spectrophotometer in 190-700 nm region, in the presence of the solvent as background. The chemical states of HNS were obtained by a VG250 X-ray photoelectron spectroscopy (VG Scientific, UK) employing Al's Kα-ray for excitation. The instrument was operated in constant analysis energy (CAE) mode with the pressure below 2×10^{-9} mbar. The FT-IR spectra of HNS samples were recorded on a Nicollet 6700 FT-IR spectrometer. For mass analysis, ionization was performed in a negative electrospray ionization mode.

The photoexcitation of HNS results in the formation of a small hole at where the laser impinged on the sample; visual inspection shows a dusting of residual black material on the windows, as shown in Fig. 3. In the UV-Vis spectra experiment, the HNS powders were dissolved into acetonitrile solvent after laser irradiation. The absorption spectrum for HNS in acetonitrile shows that the maximum absorption peak appears at 231 nm, which is attributed to the π→π* transition region of trans-stilbene, the basic chromophore group of HNS. In addition, a very small band centered at about 350 nm appears for both unirradiated and irradiated samples, which may be an artifact originating from the switching of monitor lamps in the spectrometer. After irradiation, an additional absorption peak centered at about 310 nm emerges, indicating a photochemical phenomenon.

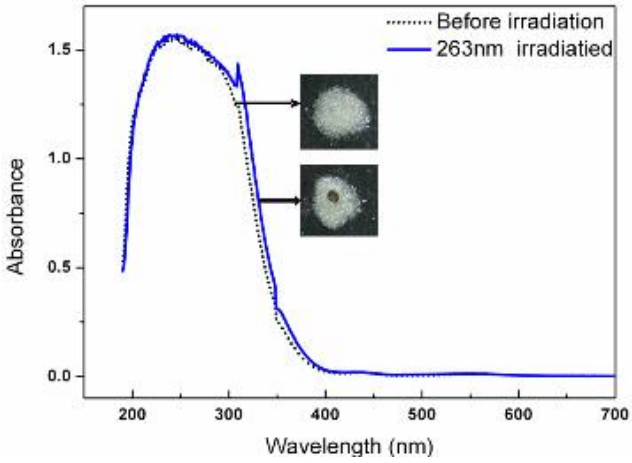

Fig. 3. UV-visible spectra of HNS before and after laser irradiation (color online)

3.2. XPS spectra

The N 1s and O 1s XPS narrow scan spectra for HNS before and after laser irradiation are shown in Fig. 4. In HNS molecule, there is no nitrogen in the ring and only one nitrogen peak arising from -NO_2 group is observed in the XPS N 1s spectra at ~405 eV before irradiation. After laser irradiation, a new peak appears at the low binding energy of 401 eV, which is attributed to the chemical state of N 1s of the nitrite ester derivative (-ONO) of HNS during the laser-induced decomposition process. A similar change is also observed for the O 1s peak. In the XPS O 1s spectra, the peaks at about 532 eV are observed for both irradiated and unirradiated samples, which are assigned to the chemical state of O 1s of the NO_2 group. After laser irradiation, a new peak appears at a lower binding energy of about 528 eV, corresponding to the chemical state of O 1s of the nitrite ester derivative of HNS. Therefore, it is concluded that the nitro-nitrite isomerization takes place in the decomposition.

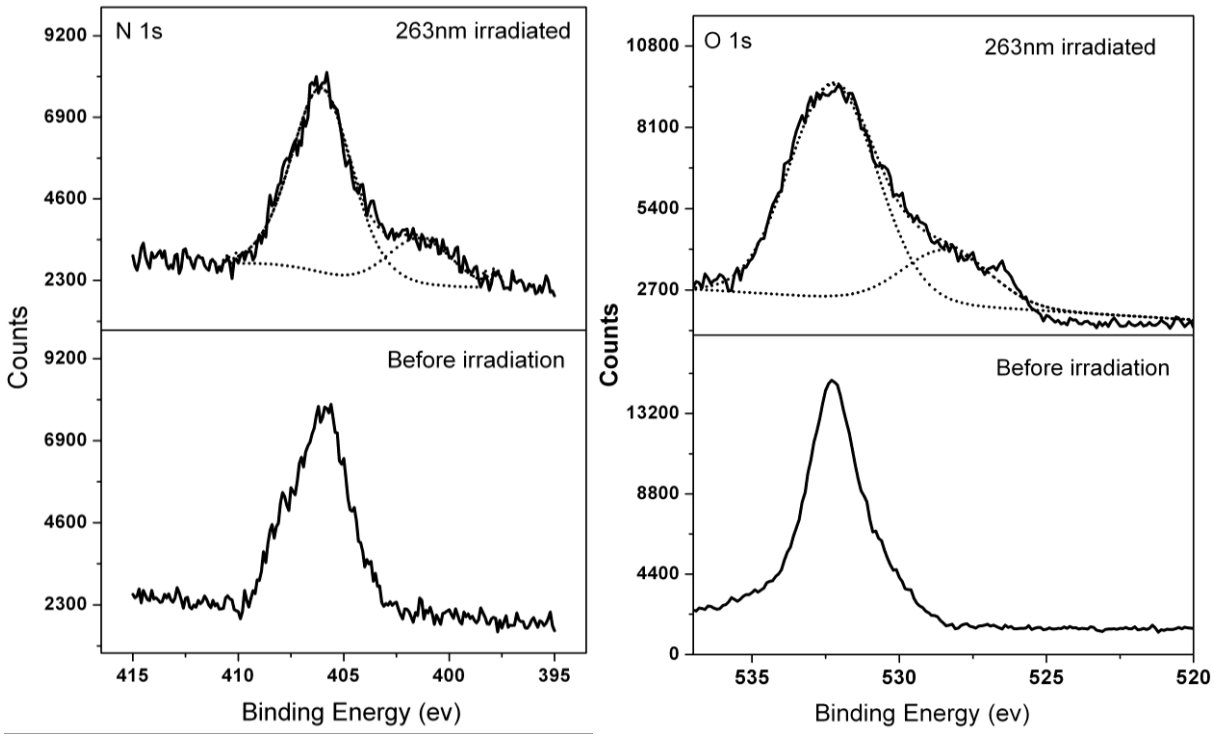

Fig. 4. XPS N 1s and O 1s narrow scan spectra of HNS before and after laser irradiation at 263 nm. The solid lines are XPS curves, the short dot lines are fitting curves

3.3. Mass spectra

In the mass spectra experiment, the HNS powders were dissolved into acetonitrile (CH_3CN) solvent after laser irradiation and the results are presented in Fig. 5. In Fig. 5, the mass peak at 279m/z is chosen as a standard and the Y axis stands for "Relative intensity". The mass peak of 449m/z and 224m/z corresponds to the parent molecule $C_{14}H_6O_{12}N_6$ and product $C_7H_3O_6N_3$, respectively. The most possible explanation of the 224m/z peak is the product due to the broken of trans-C=C bond in HNS molecule. The mass peak of 329m/z is assigned to product $C_{14}H_6O_8N_2$ after elimination of four NO groups in HNS molecule, which is related to the mechanism of nitro-nitrite isomerization with subsequent release of NO. Worth mentioned, after irradiation the relative intensity of 302m/z shows a decrease, so we cannot see the very marked peak at 302m/z after irradiation. However, a weak peak at 302m/z is still can be observed after irradiation.

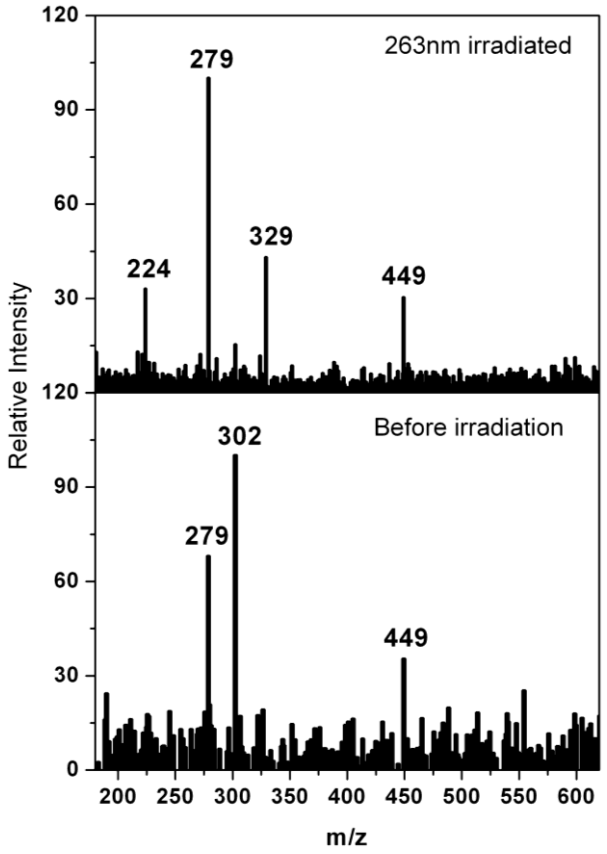

Fig. 5. Mass spectrum of HNS before and after laser irradiation

4. Discussion

Before further discussing the decomposition channels, the decomposition mechanism of HNS molecules in the present experiments should be verified. In our experiments, the energy absorbed from 263 nm decomposition laser results in electronically excited HNS molecules and then they can typically proceed down two different pathways: (1) absorbed light energy is converted to internal and translational energy, the excited molecules rapidly undergo internal conversion to the ground state with a high degree of vibrational energy from which decomposition occurs; (2) internal conversion or intersystem crossing to another excited state from which the molecule may return to the ground state or couple to a dissociative state resulting in a chemical reaction. In the first case, the molecule may be in a state that is similar to that resulting from rapid heating, which is called photothermal decomposition process. In the second case, it may induce a chemical mechanism that is unique and unlike the thermal pathway, which is called photochemical decomposition process. Generally, the photothermal and photochemical decomposition mechanisms compete in a sample and makes the explanation of experimental results difficult.

In reference [23], the authors calculated the temperature of PETN illuminated with pulsed infrared and ultraviolet radiation to estimate the extent of thermolysis. By numerically integrating the temperature equation related to time *t* and perpendicular distance *x*, they obtained the temperature change of the surface layer of PET during laser irradiation with different laser pulse. The cooling by heat conducting is also considered and depends on laser type. The temperature equation is written as

$$\frac{\partial T}{\partial t}=\frac{\kappa}{\rho C}\frac{\partial^2 T}{\partial x^2}+\frac{k_e(1-R)I(t)\exp(-k_e x)}{\rho C} \quad (1)$$

where ρ, C, and R are the density, heat capacity, and reflectivity, respectively, of HNS, $I(t)$ is the irradiance of the laser pulse and k_e is the effective absorption coefficient defined in reference [24].

Equation (1) was numerically integrated with T_0=293K initially to obtain the time dependence of the temperature at different depths within the sample. Values used in the calculation were ρ=1.74×10^3 kg·m^{-3},C=1200J·Kg^{-1}·K^{-1}, R = 0.05 and k_e =1×10^5 cm^{-1}, respectively. In the calculation, k_e is deliberately specified a high value to acquire a high temperature. Compared with an absorption coefficient of 1.15×10^4 cm^{-1} for NTO [25], k_e =1×10^5 cm^{-1} is a very high value which means a half energy losing when the laser pulse penetrates into the sample a depth of 70nm. $I(t)$ was represented by a Gaussian pulse of 8-ps (FWHM) width. For the peak power density of 10^{8}W/cm^2, the calculated temperature curve at different depths is shown in Fig. 6(a) and a specifically depth 0.1K$_e^{-1}$ (x = 10nm) below the surface of HNS is shown in Fig. 6(b), respectively. We can see the temperature decreases with x and the maximal temperature rising is less than 40K and the final temperature is much lower than the thermal decomposition temperature of HNS molecules (588K). Thus it is clearly that the thermal effect is not the dominant effect.

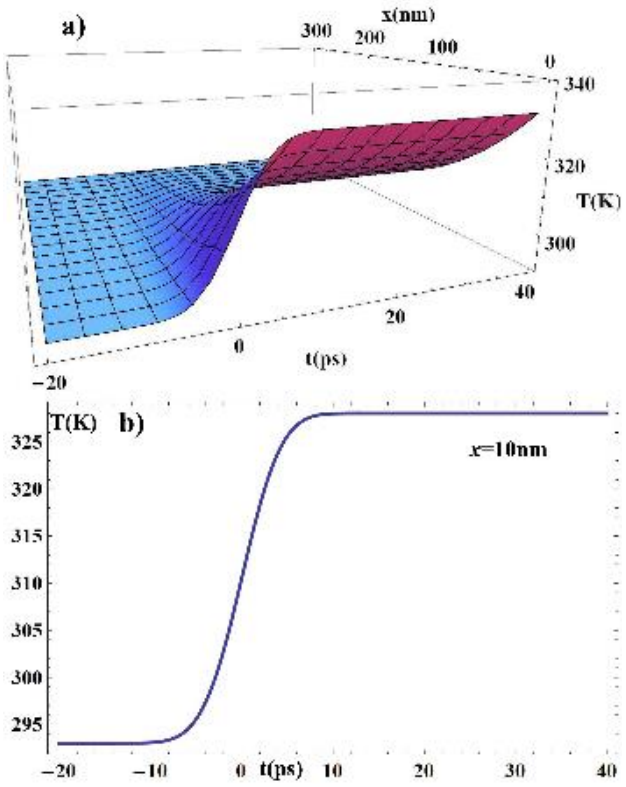

Fig. 6. Calculated temperature at different depths below the surface of HNS during UV laser irradiation with a 8-ps Gaussian pulse, F = 0.8 mJ/cm^2. a) Temperature versus different t and x; b) Temperature versus t at x=10 nm

To characterize the laser-induced decomposition steps, we have used UV-Vis spectra, X-ray photoelectron spectroscopy, and mass spectra to study the chemical structure changes of HNS after laser irradiation. The new peak at 310nm in UV-Vis spectra may be due to the n→π* transition associated with –ONO group [20]. For the XPS measurements, the appearance of the new peaks of N 1s narrow scan spectra at around ~401 eV and O 1s narrow scan spectra at about ~528 eV suggests a nitrite ester derivative (-ONO) structure of HNS due to a nitro-nitrite (NO_2-ONO) isomerization reaction. On the basis of the whole results achieved by different means, we can conclude that a nitro-nitrite (NO_2-ONO) isomerization reaction with subsequent release of NO occurs in the decomposition process. Moreover, the appearance of 224m/z mass in mass spectra verifies that the fragmentation of trans-C=C bond takes place in the decomposition. Maybe one would argue that the excited state populated by photoexcitation may access a facile pathway of fragmentation of C=C bond on the ring. However, the experimental study of photoexcitation of some simpler aromatic systems (i.e., benzene, nitrobenzene, and aniline) has demonstrated the aromatic ring is very stable. Ring cleavage in photoexcited benzene belongs to a low quantum yield process (ca.0.01-0.05) [9].

5. Conclusion

In conclusion, the laser-induced decomposition of solid HNS sample irradiated by 8 ps laser pulses at 263 nm has been investigated by UV-Vis spectra, X-ray photoelectron spectroscopy and mass spectra. The results show that the chemical structures of HNS molecules have dramatically changed due to laser irradiation. After laser irradiation, the new peak at 310nm in UV-Vis spectra and the new peak at the binding energy of 401eV of N 1s XPS spectra and 528 eV of O 1s spectra show that the nitro-nitrite isomerization with subsequent release of NO occurred in the laser-induced decomposition of HNS. The new peak at 224m/z of mass spectra indicates that the rupture of trans-C=C bond also occurs in the 8ps laser-induced decomposition of the HNS molecule. Numerically integration of the two-dimensional heat conduction equation indicates that the temperature risen of irradiated sample volume is much lower than 40K and hence the photochemical effect is the dominant reaction in the decomposition. The results may provide better control and improvement of the performance of HNS for combustion and explosion.

Acknowledgements

This work is supported by National Natural Science Fund of China (No. 11802254).

References

[1] H. Gifers, M. Pravica, J. Phys. Chem. A **112**, 3352 (2008).

[2] A. Bhattacharya, Y. Q. Guo, E. R. Bernstein, J. Phys.

Chem. A **113**, 811 (2009).
[3] Y. G. Lazarou, P. Papagiannakopoulos, J. Phys. Chem. **94**, 7114 (1990).
[4] M. J. McQuaid, A. W. Miziolek, R. C. Sausa, J. Phys. Chem. **95**, 2713 (1991).
[5] D. L. Williams, J. C. Timmons, J. D. Woodyard, K. A. Rainwater, J. M. Lightfoot, B. R. Richardson, C. E. Burgess and J. L. Heh, J. Phys. Chem. A. **107**, 9491 (2003).
[6] J. Sharma, W. L. Garrett, F. J. Owens, V. L. Vogel, J. Phys. Chem. **86**, 1657 (1982).
[7] D. Britt, W. B. Moniz, G. C. Chingas, D. W. Moore, C. A. Heller, C. L. Ko, Prop. Explos. Pyrotech. **6**, 94 (1981).
[8] J. W. Mconald, T. Schenkel, M. W. Newman, J. Energ. Mater. **19**, 101 (2001).
[9] E. A. Glascoe, J. M. Zaug, M. R. Armstrong, J. C. Crowhurst, C. D. Grant, L. E. Fried, J. Phys. Chem. A **113**, 5881 (2009).
[10] H. S. Lm, E. R. Bernstein, J. Chem. Phys. **113**, 7911 (2000).
[11] Y. Q. Guo, M. Greenfield, E. R. Bernnstein, J. Chem. Phys. **122**, 244310 (2005).
[12] M. Greenfield, E. R. Bernnstein, Y. Q. Guo, Chem. Phys. Lett. **430**, 277 (2006).
[13] Y. Q. Guo, M. Greenfield, A. Bhattacharya, E. R. Bernnstein, J. Chem. Phys. **127**, 154301 (2007).
[14] M. D. Pace, Mol. Cryst. Liq. Cryst. **156**,167 (1988).
[15] N. P. Khokhlov, N. A. Ponkin, I. A. Lukyanenko et al., Combust Explos Shock. **57**, 364 (2021).
[16] J. Hawari, S. Deschamps, C. Beaulieu, L. Paquent, A. Halasz, Water Research **38**, 4055 (2004).
[17] M. D. Pace, A. J. Carmichael, J. Phys. Chem. **101**, 1848 (1997).
[18] Yu. V. Sheikov, S. M. Bat'yanov, O. N. Kalashnikova, O. M. Lukovkin, D. V. Mil'chenko, S. A. Vakhmistrov, A. L. Mikhailov, Combust Explos Shock. **54**, 57 (2018).
[19] B. P. Aduev, D. R. Nurmukhametov, G. M. Belokurov, A. A. Zvekov, N. V. Nelyubina, Combustustion, Explosion, and Shock Waves **55**, 237 (2019).
[20] B. P. Aduev, D. R. Nurmukhametov, A. A. Zvekov, A. P. Nikitin, N. V. Nelyubina, G. M. Belokurov, A. V. Kalenskii, Tech. Phys. **64**, 858 (2019).
[21] B. P. Aduev, D. R. Nurmukhametov, N. V. Nelyubina Combustion, Explosion, and Shock Waves **55**, 718 (2019).
[22] Y. Sun, M.Shui, T. Xu, Asian Journal of Chemistry **25**, 4247 (2013).
[23] G. A. Oldershaw, Chem. Phys. Lett. **186**, 23 (1991).
[24] N. L. Garland, H. D. Ladouceur, H. H. Nelson, J. Phys. Chem. A **101**, 8508 (1997).
[25] K. J. Smit., J. Energ. Mater. **9**, 81 (1991).

*Corresponding author: 287223217@qq.com